Cancer Research

HER2 and EGFR Overexpression Support Metastatic Progression of Prostate Cancer to Bone

Kathleen C. Day[1,2,3], Guadalupe Lorenzatti Hiles[1,2,3], Molly Kozminsky[2,4,5], Scott J. Dawsey[1,2,3], Alyssa Paul[1,2,3], Luke J. Broses[1,2,3], Rajal Shah[1,6], Lakshmi P. Kunja[3,6], Christopher Hall[1,3], Nallasivam Palanisamy[3,6], Stephanie Daignault-Newton[3], Layla El-Sawy[1,2,7], Steven James Wilson[1,2,3], Andrew Chou[1,2,3], Kathleen Woods Ignatoski[1,3], Evan Keller[1,2,3], Dafydd Thomas[6], Sunitha Nagrath[2,4,5], Todd Morgan[1,3], and Mark L. Day[1,2,3]

Abstract

Activation of the EGF receptors EGFR (ErbB1) and HER2 (ErbB2) drives the progression of multiple cancer types through complex mechanisms that are still not fully understood. In this study, we report that HER2 expression is elevated in bone metastases of prostate cancer independently of gene amplification. An examination of HER2 and NF-κB receptor (RANK) coexpression revealed increased levels of both proteins in aggressive prostate tumors and metastatic deposits. Inhibiting HER2 expression in bone tumor xenografts reduced proliferation and RANK expression while maintaining EGFR expression. In examining the role of EGFR in tumor-initiating cells (TIC), we found that EGFR expression was required for primary and secondary sphere formation of prostate cancer cells. EGFR expression was also observed in circulating tumor cells (CTC) during prostate cancer metastasis. Dual inhibition of HER2 and EGFR resulted in significant inhibition of tumor xenograft growth, further supporting the significance of these receptors in prostate cancer progression. Overall, our results indicate that EGFR promotes survival of prostate TIC and CTC that metastasize to bone, whereas HER2 supports the growth of prostate cancer cells once they are established at metastatic sites. *Cancer Res; 77(1); 74–85. ©2016 AACR.*

Introduction

Prostate cancer is the most prevalent cancer in men in the United States with an estimated 180,890 new cases in 2016 and an estimated 26,120 deaths from metastatic disease (1). Significant roles for the ErbB family receptors [EGFR (HER1), HER2, HER3, and HER4] have been suggested in prostate tumorigenesis and progression for a number of years, but the molecular mechanisms by which ErbB family members support the disease progression and metastasis is not fully understood. Aberrant activities of HER2 and EGFR have also been associated with development of castration-resistant disease, possibly due to compensation for the loss of androgen signaling (2–5). Like prostate cancer, breast cancer is a hormone-sensitive/refractory disease, and both share common sites of metastases, such as bone. Importantly, adjuvant treatment with HER2 inhibitors has reduced the recurrence rate by more than 50% in women suffering from breast cancer (6). On the basis of our findings here that ErbB receptor proteins are overexpressed in metastatic prostate cancer, it may be prudent that patients suffering from advanced disease are screened for treatment with ErbB-specific inhibitors.

Although the role of HER2 in prostate cancer remains controversial (7), HER2 protein has been reported to be overexpressed during prostate cancer progression, and HER2-dependent signaling may support the development of castration-resistant prostate cancer (CRPC) by activating androgen receptor signaling through androgen ligand–independent mechanisms (5). Recent evidence supporting HER2 function in prostate cancer comes from a comprehensive immunohistochemical (IHC) evaluation of HER2 protein in a tumor array composed of 2,525 prostate cancer samples (8). This study revealed significant associations between HER2 staining and advancing stage and grade of disease and tumor recurrence with only 1 in 2,525 (0.04%) cases exhibiting HER2 gene amplification. It is also known that EGFR overexpression is associated with the development of CRPC in patients (4). However, EGFR expression is not significantly associated with tumor differentiation, positive margins, extra-prostatic invasion, or preoperative prostate-specific antigen (PSA; ref. 4), suggesting that EGFR expression only increases during disease progression and in the development of castration-resistant disease.

[1]Department of Urology, University of Michigan, Ann Arbor, Michigan. [2]Translational Oncology Program, University of Michigan, Ann Arbor, Michigan. [3]Comprehensive Cancer Center, University of Michigan, Ann Arbor, Michigan. [4]Biointerfaces Institute, University of Michigan, Ann Arbor, Michigan. [5]Department of Chemical Engineering, University of Michigan, Ann Arbor, Michigan. [6]Department of Pathology, University of Michigan, Ann Arbor, Michigan. [7]European Egyptian Pharmaceutical Industries, Alexandria, Egypt.

Note: Supplementary data for this article are available at Cancer Research Online (http://cancerres.aacrjournals.org/).

K.C. Day, G. Lorenzatti Hiles, and M. Kozminsky contributed equally to this article.

Corresponding Author: Mark L. Day, Comprehensive Cancer Center and Translational Oncology Program, University of Michigan, 1600 Huron Parkway NCRC Building 520-1348, Ann Arbor, MI, 48109. Phone: 734-763-9968; Fax: 734-647-4238; E-mail: mday@umich.edu

doi: 10.1158/0008-5472.CAN-16-1656

The most prominent site of prostate cancer metastasis is the bone, leading to a number of morbidities. Members of the ErbB family, in parallel with RANK, play an important role in bone remodeling during metastasis (9). A number of osseous tumors are believed to be driven by cell signaling pathways involving the NF-κB pathway and in particular through the recruitment of the RANK/RANKL signaling pathway (10). Recently, a connection between RANK and HER2 has been suggested whereby RANK may support ErbB2-driven tumorigenesis through the maintenance of tumor-initiating cells (TIC; ref. 11). In addition, we have demonstrated that RANK and HER2 are involved in breast cancer bone metastasis (12). RANK, like HER2, has been implicated in cellular migration and plasticity and has emerged as a target receptor on the surface of breast cancer stem cells (13).

The intermediate state between primary and metastatic tumors and their ultimate metastases are circulating tumor cells (CTC), those cells that are shed and present in the blood stream (14). The clinical significance of CTCs has been shown in multiple cancers, including prostate cancer, in which the prognostic values of CTC counts above and below the cutoff of 5 CTCs/7.5 mL whole blood have been associated with overall survival (15). Beyond enumeration, novel CTC isolation technologies have also enabled further characterization, including protein expression by immunofluorescence (16, 17).

In the current study, we evaluated the expression of HER2 protein in metastatic samples obtained from patients with prostate cancer and investigated the functional significance of HER2 and EGFR overexpression in the osseous growth of human prostate cancer cells *in vivo*. The role of EGFR was also examined in the tumor-initiating population of prostate cancer cells, where it may support their survival and promote self-renewal in the bone microenvironment. In addition, results from patient samples suggest that EGFR may also have a role in the survival of CTCs in the metastatic progression of prostate cancer.

Materials and Methods

Cell culture and inhibitors

LNCaP, MCF7, BT-474, and SK-BR-3 were purchased from ATCC. C4-2B and C4-2B luciferase transduced (C4-2B^{Luc}) cell lines were obtained as previously described (18). All cell lines, including luciferase and knockdown cell lines, were fingerprinted (IDEXX RADIL). Cell lines were cultured in DMEM (Lonza), RPMI-1640 (Mediatech), 50% DMEM/50% RPMI, or T-Medium (Gibco), supplemented with 10% FBS (HyClone), penicillin/streptomycin/Fungizone, and L-Glutamine (Gibco). Cells were kept in a 37°C, 5% CO_2-humidified incubator. Lapatinib and afatinib were purchased from LC Laboratories. Cetuximab and trastuzumab were obtained from the Cancer Center Pharmacy, University of Michigan (Ann Arbor, MI). For the generation of lentiviral vectors and stable cell lines, see Supplementary Data.

Animal models and treatments

All experiments began with 8-week-old male NOD/SCID mice from Jackson Laboratories. Mice received (right) tibia injections of 5×10^5 C4-2B cells containing either shVector ($n = 10$) or shHER2 ($n = 10$). After 3 weeks, the mice were sacrificed and tibiae (right and left) were removed and fixed in 10% formalin. For the inhibitor experiments, each mouse ($n = 30$) received an intratibial injection of 1×10^6 C4-2B^{Luc} cells in their right tibia. Drug treatments started the following day for lapatinib ($n = 10$) and trastuzumab + cetuximab dual treatment groups ($n = 10$). Untreated control mice ($n = 10$) had the same tibia xenografts. Lapatinib was given orally at 100 mg/kg 5 times per week. The inhibitor cocktail [trastuzumab (10 mg/kg) + cetuximab (3 mg/kg)] was given by intraperitoneal (i.p.) injections 3 times per week. After 7.5 weeks of treatment, the mice were sacrificed and tibiae collected in 10% formalin. These experiments were based on reports of dose escalation of lapatinib (19–21) and on combinations of inhibitors (22). All animal experiments were approved by the Institutional Animal Care and Use Committee.

IHC and tissue microarrays

Prostate cancer tissue microarray (TMA) slides were designated TMA 85 (primary and bone) and TMA 142 (primary, lymph node, and liver). TMAs were prepared as previously described (23, 24). Formalin-fixed, paraffin-embedded (FFPE) tissue blocks with tumor samples were previously identified by a pathologist and processed as instructed by the IRB. Prostate tissue samples were taken from the radical prostatectomy series and the University of Michigan SPORE Rapid Autopsy Program (25). Tumors were staged and graded using the Gleason system (26). All tissue sections were reviewed by 2 board-certified genitourinary pathologists (R. Shah, L.P. Kunja) and scored for stain intensity (0–3), percent positivity, and subcellular location.

The tibiae from the mice were decalcified in Decalcifier II (Leica Biosystems) for 3 hours before paraffin embedding. Antigen retrieval was performed for NeoMarkers' staining by pretreating with citrate at pH 6 with microwaving for 10 minutes, cooled for 10 minutes, and washed with water for 10 minutes. There was no pretreatment for Dako staining, which was stained using the Dako AutoStainer. All tissue sections were cut to 4-μm thickness. Hematoxylin and eosin (H&E) staining was analyzed, followed by IHC for the following biomarkers in serial sections: anti-HER2 (NeoMarkers Ab-17 1:100), anti-HER2 (Abcam EP1045Y 1:100), anti-HER2 (Dako A0485 manufacturer spec.), anti-EGFR (Life Technologies 31G7 1:100), anti-CK8/18 (Epitomics ac-9002RUO 1:100), anti-pHist3 (Abcam ab5176 1:500), anti-RANK (R&D Systems 80707 1:500), anti-Ki-67 (Dako MIB-1 1:200), and anti-E-cadherin (ThermoFisher HECD-1 1:200). For details on tissue imaging, see Supplementary Data.

Cell viability assay

Five thousand C4-2B cells were seeded per well into 96-well plates, and 24 hours later, lapatinib was added to reach the indicated concentrations. The Titer Blue reagent (CellTiter-Blue Cell Viability Assay, Promega) was used to detect cell viability at 1, 24, and 48 hours of treatment using a fluorescent plate reader (Molecular Devices tunable SpectraMax M5). This assay was conducted as per the manufacturer's instructions.

Western blotting

Protein isolation and Western blotting were carried out as previously described (27), with these primary antibodies: anti-HER2 (NeoMarkers Ab-17) anti-HER2 (Abcam EP1045Y), anti-EGFR (NeoMarkers H9B4), anti-α-tubulin (Upstate DM1A), and anti-E-cadherin (ThermoFisher HECD-1). Mouse and rabbit HRP-conjugated secondary antibodies (Bio-Rad) were used and

illuminated by ECL (Advansta). One Western blot assay utilized IRDye 680 goat anti-mouse and IRDye 800 goat anti-rabbit secondary antibodies (LI-COR).

Quantitative flow cytometric analysis

Cell surface HER2 and EGFR were quantified using the Dako QIFIKIT according to the manufacturers' protocol. Three different passages of C4-2B cells were grown in complete T-medium without phenol red and detached with TrypLE Express (Gibco). A total of 1×10^5 C4-2B cells were analyzed in triplicate. HER2-binding sites were saturated with anti-HER2 (R&D Systems 191924; 10 μg/mL) and EGFR sites with anti-EGFR (LSBio 225; 10 μg/mL) as primary antibodies. Alexa Fluor 488 goat anti-mouse IgG (H+L) (Invitrogen; 1:400) was utilized as the secondary antibody. The median fluorescence intensity (MFI) was analyzed by flow cytometry (Accuri BD analyzer) and the number of molecules per cell calculated by FlowJo and subsequent extrapolation of the samples' MFI into a standard curve on the basis of the calibration beads MFI.

Cell staining and prostate tumor sphere (prostasphere) formation

C4-2B cells were prepared as described for "QIFIKIT analysis" and profiled by FACS with fluorescent-labeled anti-EGFR FITC (Abcam ICR10 1:40), anti-HER2 APC (B.D. Neu24.7 1:133), and anti-RANK PE (Abcam 9A725 1:17) antibodies. Live cell staining of 1×10^6 cells (per analysis) was carried out in staining buffer (RPMI no phenol red with 2% FBS) in a final volume of 200 μL. Cells were stained for 1 hour on ice plus 10 minutes at room temperature, washed with 2 mL of staining buffer, filtered through cell strainer–capped tubes (Falcon 352235), and then resuspended in 250 μL of staining buffer with DAPI. FACS was carried out as described previously (12), and cells were sorted directly into T-Medium. The MoFlo XDP instrument was utilized for the analysis. DAPI was added for selection of viable (vs. DAPI-negative) cells where DAPI-positive cells (no antibody staining) were sorted as viable controls for sphere formation. For positive cell staining: $EGFR^{high}$ (top 5%), $EGFR^{low}$ (bottom 5%), $HER2^{high}$ (top 5%), $HER2^{low}$ (bottom 5%), RANK-positive, and RANK-negative cells were collected and seeded in triplicate at 200 cells/200 μL (96-well plates) in complete MammoCult medium (STEMCELL Technologies). Primary prostaspheres were grown for 10 days followed by disruption with trypsin and then reseeded (200 cells/200 μL of MammoCult medium) to develop secondary spheres after another 10 days of growth. Spheres were viewed using an Olympus CKX41inverted microscope.

FISH

An *ERBB2* BAC probe, which encoded for the entire gene sequence of the *ERBB2* gene (introns and exons), was utilized for gene copy number analysis. Labeled probe was generated by DNase treatment of the *ERBB2* gene and Nick translation incorporated Dig-dUTP nucleotides into dsDNA. *ERBB2* cDNA was denatured by heat treatment at 75°C to produce single-strand DNA probe. Fixed tissues (on slides) were denatured with formamide at 42°C prior to hybridization with labeled probe. Fluorescent antibody to Dig-dUTP was employed for imaging and analysis.

In vivo tumor imaging with firefly luciferase bioluminescence

Mice received intraperitoneal injections of 2-mg D-luciferin and were anesthetized. Ten minutes after the injection, the luciferase signatures were captured using a PerkinElmer IVIS Spectrum with Living Image software (v4.2).

CTC isolation using graphene oxide chip

CTCs were isolated from whole blood samples taken from consented patients with prostate cancer under IRB: HUM52405. Procedures for microfluidic chip fabrication and CTC isolation using the microfluidic graphene oxide (GO) chip have been described elsewhere (16). Briefly, tetrabutyl ammonium hydroxide–intercalated GO nanosheets grafted with phospholipid-polyethyleneglycol-amine were assembled on gold-patterned silicon substrates and enclosed in a polydimethylsiloxane (PDMS, Dow Corning Sylgard) chamber. Components of a functionalization chemistry could then be introduced to the assembled device via Harvard Apparatus syringe pump to ultimately present an antibody against the epithelial cellular adhesion molecule, anti-EpCAM (R&D Systems). Whole blood was flowed through the device to enable CTC capture, after which the device was washed and the cells were fixed. Cells were then permeabilized and stained on-chip with primary antibodies against cytokeratin 7/8 (CK, BD Biosciences CAM5.2), CD45 (Santa Cruz 3H1363), and EGFR (Invitrogen 31G7) with the appropriate secondary antibodies (Invitrogen) and the nuclear stain DAPI (Invitrogen). Devices were scanned using a Nikon TI inverted fluorescence microscope. Nucleated $CK^+/CD45^-$ entities were enumerated as CTCs.

Statistical analysis

Results of *in vitro* experiments are presented as mean ± SD or mean ± SE. The Student *t* test was used to compare continuous variables when there were 2 groups. A paired *t* test was used for paired data comparisons. Mouse tumor xenografts experiments are presented with means and SEs of the mean. Pairwise comparisons were made using ANOVA within the models at cross-sections and the Bonferroni multiple comparisons adjustment was used for pairwise tests. Analyses were completed using SAS 9.3 (SAS Institute). The mean values between prostasphere groups were compared in ANOVA by Tukey multiple comparisons using GraphPad Prism 6.0 (GraphPad Software, Inc.). Alpha of 0.05 determined statistical significance.

Results

HER2 protein is overexpressed in organ-confined prostate cancer

It is known that EGFR is overexpressed in metastatic and CRPC (4); however, the evaluation of HER2 protein at this stage of prostate cancer has not been investigated. Mechanisms of HER2 overexpression have historically been explained in the context of gene amplification, whereas transcriptional and posttranscriptional mechanisms leading to increased HER2 protein have not been critically evaluated. We utilized two distinct HER2 antibodies: the first, a cytosolic-specific polyclonal antibody (Dako); and the second, two monoclonal antibodies that recognize two cytosolic epitopes (NeoMarkers). Both antibodies were used to evaluate HER2 protein in FFPE sections of normal prostate, localized prostate cancer, and metastatic prostate cancer. We evaluated H&E-stained serial sections (Fig. 1A, i and ii) followed by staining with the

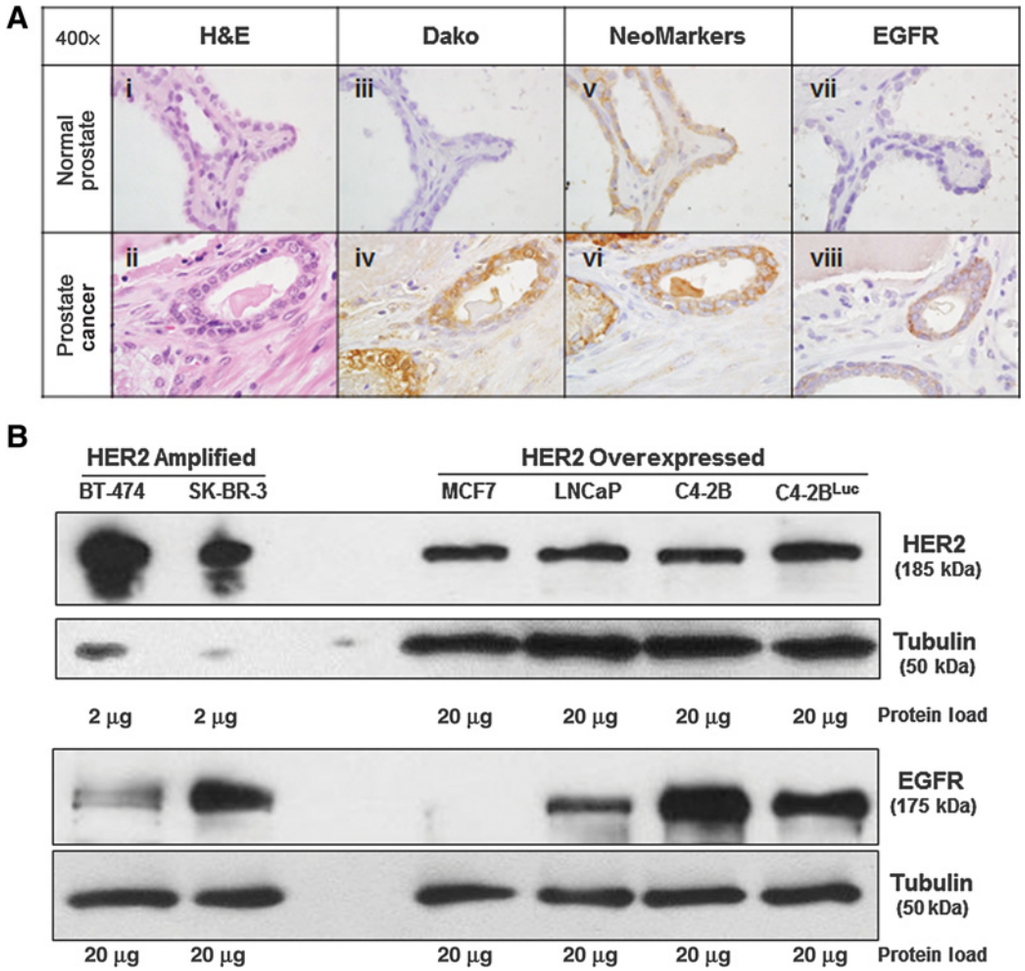

Figure 1.

HER2 and EGFR are overexpressed in advanced prostate cancer. **A,** Serial sections of normal prostate (**i, iii, v, vii**) and prostate cancer (**ii, iv, vi, viii**) were stained with H&E, Dako (Rb.pAb anti-HER2), NeoMarkers (MAb anti-HER2), and ab-15 (MAb anti-EGFR). **B,** Western blot analysis of breast cancer (BT-474, SK-BR-3, MCF7) and prostate cancer (LNCap, C4-2B, C4-2B^{Luc}) whole-cell lysates at either 2 µg (HER2-amplified) or 20 µg of cellular protein. Tubulin was used as a loading control.

indicated HER2 antibodies (Fig. 1A, iii–vi). A direct comparison of both antibodies revealed that the Dako antibody does not detect HER2 protein in normal prostate, but that the NeoMarkers antibody detects low levels of HER2 located at the basal–lateral junctions of luminal epithelium (Fig. 1A, iii and v). Both HER2 antibodies detected elevated protein in prostate cancer tissue (Fig. 1A, iv and vi), and we found that EGFR was expressed in moderate levels in localized (primary) cancer (Fig. 1A, vii and viii). The cytosolic epitopes of both HER2 antibodies and their relative affinity for HER2 are shown schematically in Supplementary Fig. S1. The Dako polyclonal antibody was designed as a diagnostic reagent to detect high levels of HER2 protein in breast cancer specimens containing *ERBB2* gene amplification. The more sensitive NeoMarkers antibody is able to detect HER2 protein from both amplified and nonamplified sources in paraffin-embedded tissue. To demonstrate the range of sensitivity of the NeoMarkers antibody, we analyzed HER2 protein levels by Western blot analysis from lysates of the *ERBB2*-amplified breast cancer lines BT-474 and SK-BR-3 and compared these to HER2 protein levels from 10-fold greater loadings of the nonamplified MCF7 breast cancer cells and nonamplified LNCaP and C4-2B prostate cancer cells (Fig. 1B). In addition, we evaluated EGFR protein levels from these same lysates and found that EGFR is strongly overexpressed in the androgen-insensitive C4-2B subline compared with its parental line, LNCaP (Fig. 1B).

Assessment of HER2 in localized and metastatic prostate cancer

A 17-patient prostate cancer metastasis TMA (TMA 85) was stained with the Dako and NeoMarkers HER2 antibodies (Fig. 2A and B). An intensity score (0–3) was assigned to the stained core by 2 board-certified genitourinary pathologists (R. Shah and L.P. Kunja). Examination of TMA 85 revealed that the more sensitive NeoMarkers antibody exhibited a significantly higher percentage of staining where 75.57% of all cores scoring 2+3+ compared with a mean staining of 40.99% scoring 2+3+ with the Dako antibody. NeoMarkers stained 92% of the bone cores with 2+3+ intensity scores. In contrast, the Dako antibody stained 46% of the

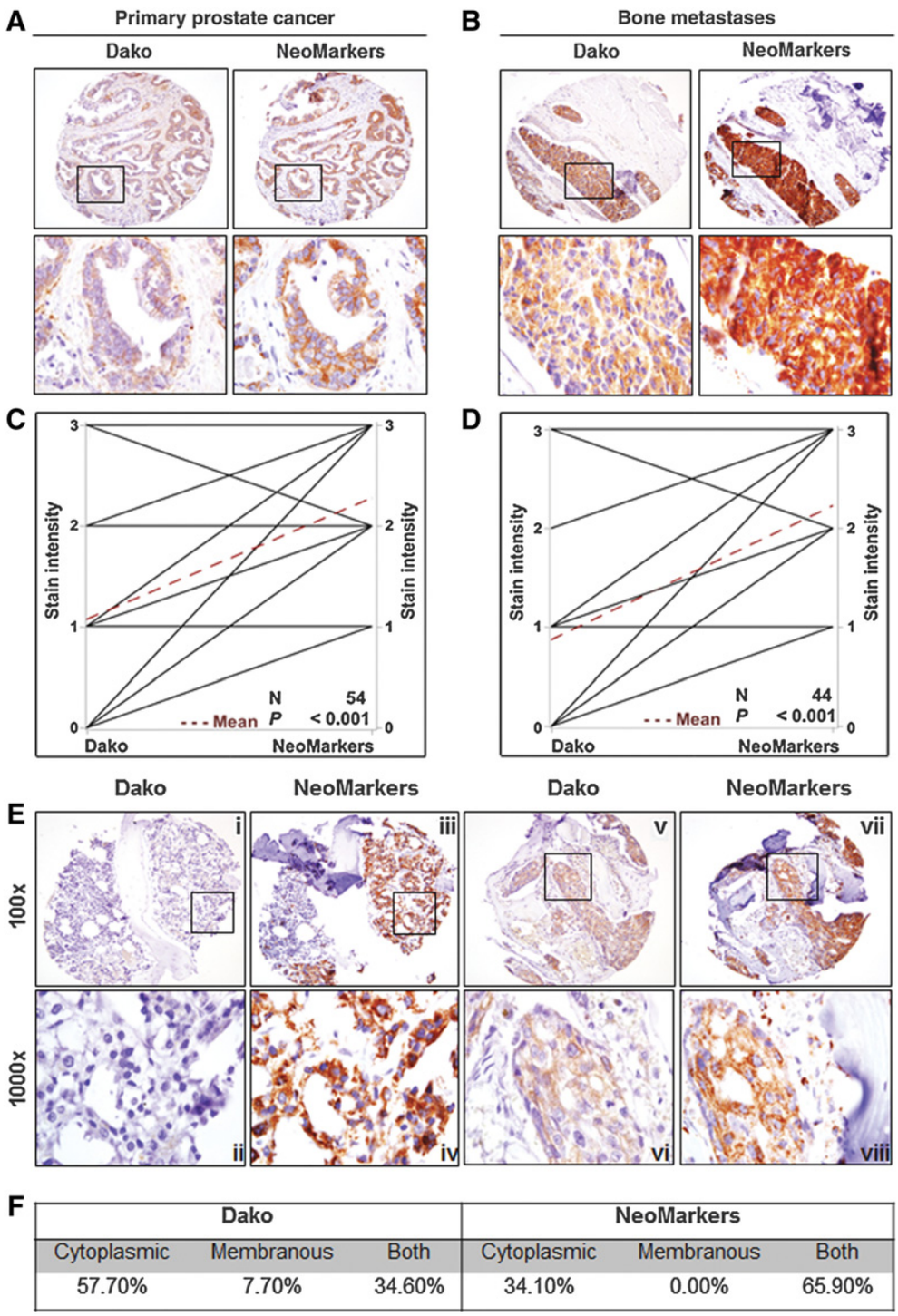

F

Dako			NeoMarkers		
Cytoplasmic	Membranous	Both	Cytoplasmic	Membranous	Both
57.70%	7.70%	34.60%	34.10%	0.00%	65.90%

Figure 2.
Evaluation of HER2 staining in a prostate cancer metastasis TMA. **A,** IHC staining of primary prostate cancer. **B,** Bone metastases from serial sections of TMA 85 with Dako and NeoMarkers antibodies All of the cores (**C**; $n = 54$) and bone cores (**D**; $n = 44$) from TMA 85 were graphed to compare Dako stain intensity to NeoMarkers stain intensity in a paired analysis ($P < 0.001$). **E,** Two different patients' bone cores from TMA 85 stained with Dako and NeoMarkers antibodies. Inset boxes (**ii, iv, vi, viii**) are 1,000× magnification of ×400 images (**i, iii, v, vii**). **F,** Tabulated summary of cellular distribution of HER2 staining on TMA 85.

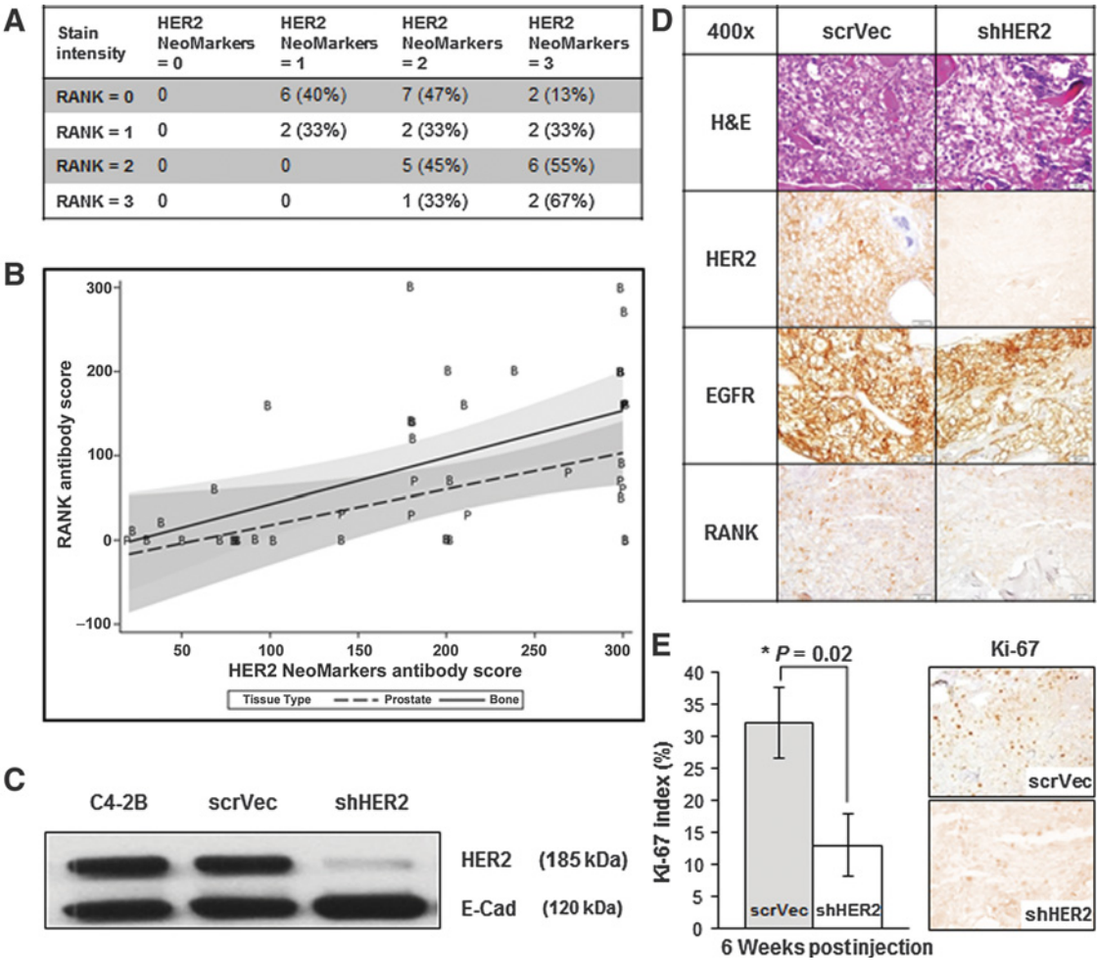

Figure 3.

Characterization of HER2 knockdown in C4-2B prostate cancer intratibial xenografts. **A** and **B,** Tabulated results (**A**) of scatter plot (**B**) with regression lines of TMA 85 stained for HER2 and RANK. **C,** Western blot analysis of HER2 expression in C4-2B parental, scrVec, and shHER2 cells. E-Cadherin was used as a loading control. **D,** SCID mouse model of tibiae injections of shHER2 versus scrVec C4-2B cells. Representative IHC of the tibiae at 3 weeks post injection using H&E, anti-HER2 (NeoMarkers), anti-EGFR, and anti-RANK. **E,** From these same mice tibiae, Ki-67 staining was assessed by counting 5 × 100 cells and using the average percent positive. *, $P = 0.02$.

bone cores 2+3+. The difference in staining intensity (Fig. 2C and D) reflects the antibody characteristics described in Supplementary Fig. S1. Shown in Fig. 2E (core 1: i–iv and core 2: v–viii) are serial sections of 2 representative patients with bone metastasis from the metastasis array to characterize the cellular location of HER2 staining with these antibodies. Cellular localization of HER2 staining in the bone metastasis cores is described as cytoplasmic, membranous, or as a combination of both (Fig. 2F). The Dako antibody exhibited primarily cytosolic staining in organ-confined disease (Fig. 2A) and retained this pattern in bone metastasis (Fig. 2B and E). Interestingly, the staining for the NeoMarkers antibody changed from a predominantly membrane pattern in early-stage disease (Fig. 2A) to an intense cytosolic pattern in bone metastasis (Fig. 2B and E). As in previous experiments, the NeoMarkers antibody appears more sensitive for the detection of HER2 *in situ* than the Dako antibody. FISH analysis was performed on TMA 85 and TMA 142, another prostate cancer array with 49 patients, to determine whether *ERBB2* gene amplification was present. In agreement with the FISH analysis of radical prostatectomy specimens reported by Minner and colleagues (8), all 35 patients' TMAs had normal *ERBB2* copy numbers, thus eliminating gene amplification as a mechanism of HER2 and EGFR protein overexpression (Supplementary Fig. S2).

Association of RANK and HER2 expression in bone metastasis and the requirement of HER2 for osteoblastic growth

The RANK-mediated NF-κB signaling axis is believed to regulate HER2 expression (28) in supporting cancer stem cells in murine models of HER2-expressing breast cancer (29). RANK regulation of HER2 may also be important in the metastatic progression of both breast and prostate cancers (28). Prostate cancer cells with activated RANK-mediated signaling networks are thought to recruit and possibly drive prostate cancer cells to participate in bone and soft tissue colonization (30). To determine whether a positive relationship exists between RANK and

HER2 expression, we stained serial sections of TMA 85 (metastasis array) with an anti-human RANK antibody and the HER2 NeoMarkers antibody. The HER2 NeoMarkers staining positively correlated with RANK staining (Spearman correlation = 0.767 as shown in the scatter plot of the stains; Fig. 3A and B). The HER2 Dako staining also positively correlated with RANK staining (Spearman correlation = 0.55, graph not shown) but to a lesser extent than NeoMarkers. Next, to determine whether HER2 protein is required for the osseous growth of prostate cancer cells, we knocked down *ERBB2* mRNA in C4-2B cells using lentiviral constructs containing *ERBB2*-specific shRNA sequences (shHER2) or scrambled *HER2* sequences (scrVec). Reduction of *ERBB2* was confirmed by Western blot analysis of shHER2 C4-2B cells compared with scrVec and parental (no transduction) control cells (Fig. 3C). scrVec or shHER2 C4-2B cells were injected into the tibia of male SCID mice and allowed to grow for 5 weeks, at which time the tibiae were prepared for IHC analysis. The NeoMarkers antibody in scrVec and shHER2 tumors confirmed that the loss of HER2 expression was maintained in the knockdown xenografts *in vivo* (Fig. 3D). EGFR levels were unchanged in these tumors. However, levels of the proliferation marker, Ki-67, were reduced in parallel with the reduction in HER2 protein expression

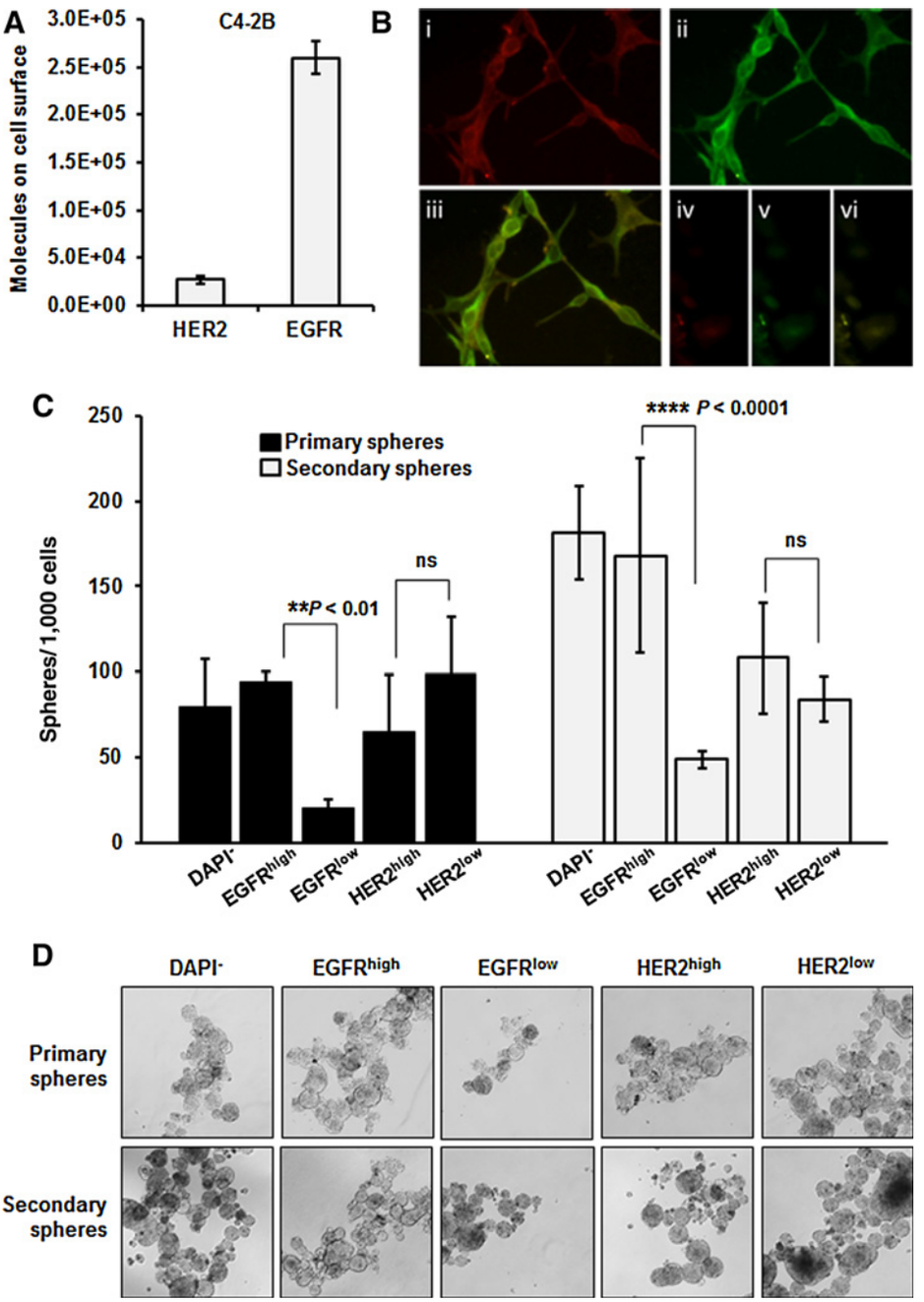

Figure 4.
The impact of EGFR and HER2 levels on prostate sphere formation. **A,** Flow cytometric quantification of EGFR and HER2 molecules on the surface of C4-2B cells under normal growth conditions. **B,** Fluorescent microscopy of costained C4-2B cells: **i,** anti-HER2; **ii,** anti-EGFR; **iii,** EGFR and HER2 colocalization; and **iv–vi,** the respective staining backgrounds. **C,** C4-2B cells were sorted via flow cytometry for high or low expression of EGFR or HER2 (independently). The sorted cells were grown as primary and secondary prostate spheres and then quantified. Cells expressing low levels of EGFR were significantly inhibited in their capacity to form primary and secondary prostaspheres than cells expressing high levels of EGFR. The results represent the mean ($n = 3$) of 1 of 3 independent experiments. **, $P \leq 0.01$; ****, $P \leq 0.0001$; ns, not significant ($P > 0.05$). **D,** Brightfield photographs (×10) of the primary and secondary C4-2B prostaspheres as analyzed in **C**.

(Fig. 3E), indicating reduced cellular proliferation in these bone xenografts.

The role of EGFR and HER2 in prostasphere formation

To determine whether HER2 or EGFR plays a regulatory role in the tumor-initiating component of prostate cancer metastasis, we quantified HER2 and EGFR cell surface expression in C4-2B cells by flow cytometry (Fig. 4A). The amount of EGFR (260,000 molecules/cell) on the cell surface was 10-fold higher than HER2 (27,000 molecules/cell) on C4-2B cells. This difference could be visualized by weak cell surface immunofluorescence using an HER2-specific antibody (Fig. 4B, i) compared with strong cell surface immunofluorescence using an EGFR-specific antibody (Fig. 4B, ii). We next examined sphere formation in cells that were selected from the top 5% of EGFR or HER2 surface expression in comparison with cells selected for the lowest 5% of EGFR or HER2 surface expression (Supplementary Fig. S3A). Only high EGFR expressing cells were able to produce primary spheres compared with the DAPI-negative or viable control cells (Fig. 4C and D). In addition, the ability of C4-2B cells to form primary spheres was only reduced in low EGFR-expressing cells. There was no independent requirement for HER2 expression for primary sphere formation, as HER2^{low} cells were fully capable of sphere formation (Fig. 4C and D). Interestingly, RANK was not required for sphere formation as high and low RANK-expressing cells did not differ in their capacity to form primary and secondary spheres (Supplementary Fig. S3B and S3C). To confirm that high EGFR expression was important for the tumor-initiating potential of C4-2B cells, we performed secondary sphere formation assays, which validated the association of high EGFR protein on cell surface and the ability to form secondary spheres (Fig. 4C and D). Because sphere-propagating cells have been associated with tumor-initiating or stem cell–like properties in prostate cancer cells (31–34), our findings support the idea that EGFR may mediate prostate cancer metastasis by supporting the TICs.

EGFR is expressed on CTCs from patients with bone metastasis

CTCs may share important characteristics with cancer stem cells, such as the capacity for dormancy and the expression of a variety of growth factor receptors, including HER2 and EGFR (35–38). To determine whether EGFR is expressed on CTCs in patients with prostate cancer bone metastasis, we isolated CTCs

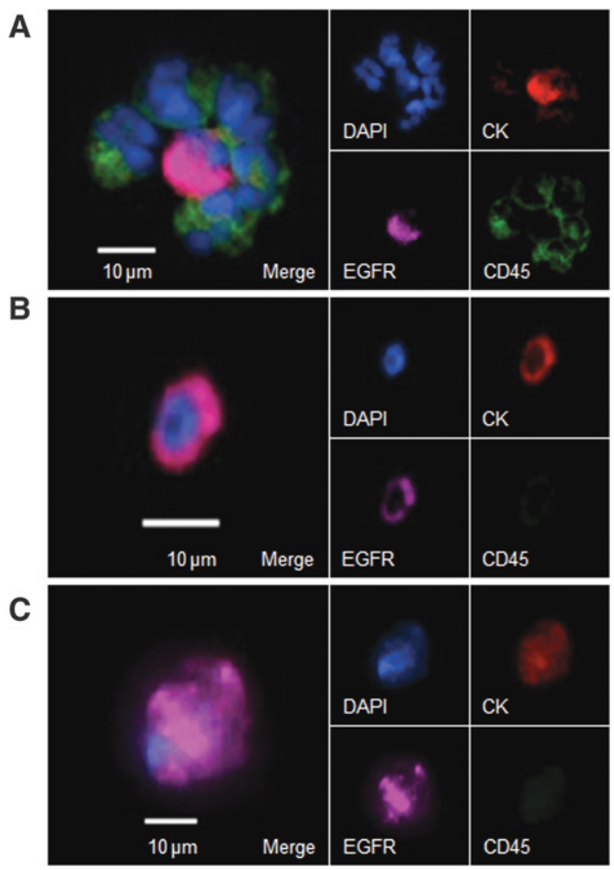

D

	N	%
Number of patients	10	100%
Age		
Median (range)	67.5	(57-77)
Castrate resistant	10	100%
Prostatectomy	4	40%
Prostate-specific antigen		
Median (range)	7.25 ng/mL	(0.09-346.7 ng/mL)
Gleason score		
Median (range)	7	(6-9)
Disease involvement		
Bone only	8	80%
Bone plus soft tissue	2	20%
Hormonal therapies	10	100%
Targeted agents	2	20%
Chemotherapy	3	30%
Radiation	9	90%

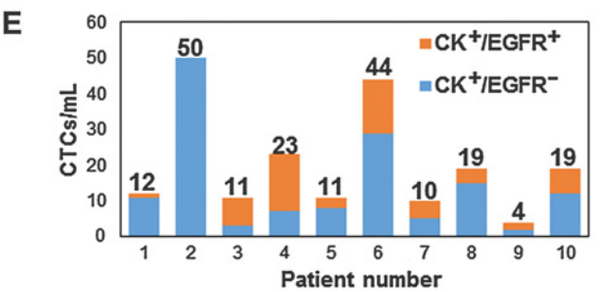

Figure 5.

Analysis of CTCs from 10 patients with metastatic prostate cancer. **A,** Cluster of white blood cells surrounding a $CK^+/EGFR^+$ CTC from patient 3. White blood cells stained positive for CD45. **B** and **C,** Other representative images of $CK^+/EGFR^+$ CTCs from patients 3 and 5 respectively. **D,** Clinical history of patients with prostate cancer analyzed for CTCs. **E,** Number of $CK^+/EGFR^+$ and $CK^+/EGFR^-$ CTCs isolated per 1 mL whole blood. Numbers above the columns indicate the total number of CTCs isolated from patients 1–10.

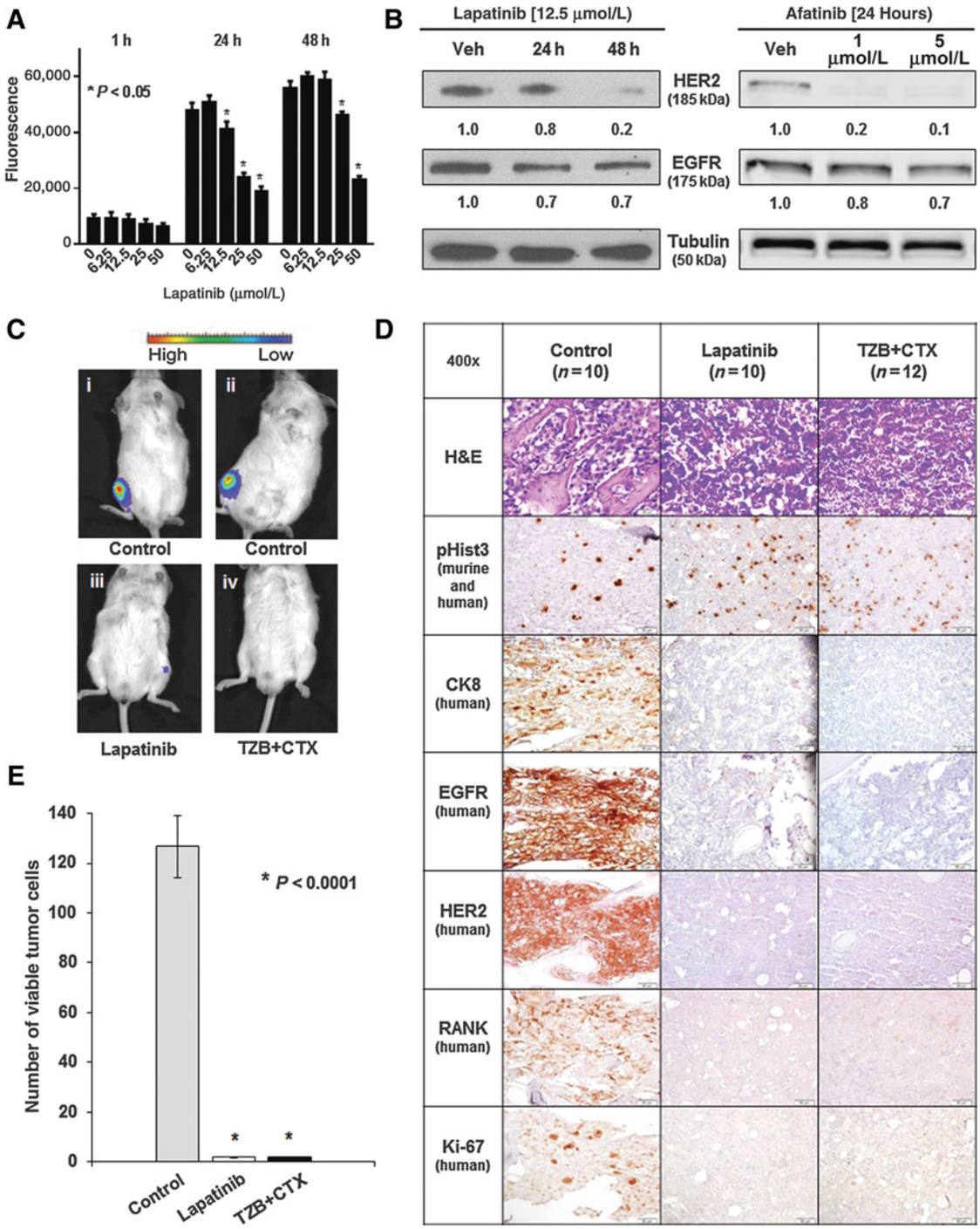

Figure 6.

Pharmacologic inhibition of HER2 and EGFR is cytotoxic to prostate cancer *in vitro* and prevents cancer growth *in vivo*. **A,** C4-2B^{Luc} cell viability measured by Titer Blue following lapatinib treatment for 1, 24, and 48 hours. *, $P < 0.05$ compared with vehicle control. **B,** Left, Western blot analyses of HER2 and EGFR expression in C4-2B cells following incubation with vehicle or 12.5 μmol/L lapatinib at 24 and 48 hours. Right, Western blot analysis of C4-2B^{Luc} cells after incubation with vehicle, 1 μmol/L, or 5 μmol/L afatinib for 24 hours. Tubulin was used as a loading control. Left, densitometry was performed with ImageJ. Right, fluorescence was measured using the Odyssey CLx (LI-COR) and quantified using Image Studio v3.1.4 software (LI-COR). Both, normalized to tubulin, values shown under respective lanes. **C** and **D,** C4-2B^{Luc} cells were injected into mouse tibiae 1 week prior to treatments. Untreated mice (Control, $n = 10$), treated with lapatinib ($n = 10$), or treated with a combination of trastuzumab and cetuximab (TZB + CTX, $n = 12$) biweekly for 6 weeks. **C,** Bioluminescence of representative mice at the end of the study where **i** and **ii** are control, while **iii** and **iv** received dual inhibitor treatments. **D,** Serial sections of representative tibia stained with H&E, anti-pHist3, anti-CK8, anti-EGFR, anti-HER2, anti-RANK, and anti-Ki-67. **E,** Quantitation of viable tumor cells was performed by counting three fields of anti-CK8–positive cells in areas that exhibited Ki-67 positivity in three animals per group. No viable human tumor cells could be found in the lapatinib or in the TZB + CTX groups at 7.5 weeks. *, $P < 0.0001$.

from whole blood samples taken from consented patients with prostate cancer using the microfluidic GO chip (16). An antibody against the epithelial cellular adhesion molecule (anti-EpCAM, R&D Systems) was used for CTC capture (protocol is depicted in Supplementary Fig. S4), and captured CTCs were then stained on-chip with primary antibodies against cytokeratin 7/8 (CK), CD45, and EGFR (Fig. 5A–C). The clinical characteristics of the 10 patients are described in Fig. 5D. All patients exhibited metastatic disease with significant bone involvement. CTCs were present in all 10 patients and EGFR staining was detected on CTCs in 9 of 10 patients. A median of 35.5% of CTCs were positive for EGFR staining (Fig. 5E).

Dual inhibition of EGFR and HER2 is cytotoxic to C4-2B cells in culture and in intratibial xenografts

The observation that EGFR protein expression was unchanged in viable HER2-knockdown cells coupled with the finding that reduction of EGFR expression was lethal in C4-2B cells suggested a role for EGFR in the survival of prostate cancer cells. C4-2B cells exhibited dose-dependent sensitivity to the pan-ErbB tyrosine kinase inhibitor lapatinib over 48 hours (Fig. 6A). The efficacy of lapatinib and afatinib, a related EGFR/HER2 tyrosine kinase inhibitor, on the C4-2B cells was associated with a reduction of both HER2 and EGFR protein following treatment (Fig. 6B). To further assess a dual role for HER2 and EGFR in survival, C4-2B luciferase–expressing xenografts were established in NOD/SCID mice. Thirty-four mice were randomized into 3 treatment groups and monitored by bioluminescence over 7 weeks. Treatment with lapatinib or a combination of cetuximab (anti-EGFR) and trastuzumab (anti-HER2) resulted in smaller tumors at 7.5 weeks posttreatment (Fig. 6C and E). Significant changes in the expression of several relevant biomarkers were also noted in the drug-treated xenografts (Fig. 6D). A reduction in HER2 and EGFR staining reflected target-specific cytotoxicity of the C4-2B cells, whereas loss of CK8 and RANK revealed that these human tumor cells were completely depleted in the tibiae. We observed a near-complete reduction of cellular proliferation in the shHER2 C4-2B bone xenografts as reflected by loss of Ki-67 staining (Fig. 6D and E). Positive staining for murine phospho-Histone H3 (pHist3) indicates that after treatment, there are still proliferating mouse cells in the marrow. The lack of EGFR- and HER2-positive cells suggests that ErbB targeting agents have very pronounced efficacy on prostate cancer in the tibia xenograft model. This is supported by the H&E stains that show the dual treated tibiae have noticeably less tumor cells (Supplementary Fig. S5).

Discussion

Metastatic prostate cancer is a deadly disease that initially responds to docetaxel-based chemotherapy and drugs that suppress androgen signaling. While these treatments may offer temporary relief, relapse is inevitable, and therapeutic options for treating patients who fail primary treatment are very limited. Thus, the search for new therapeutic strategies to treat advanced prostate cancer remains of paramount importance. A promising area of investigation focuses on inhibiting specific growth factor signaling pathways that directly support the metastatic progression of prostate cancer. Alterations in growth factor receptors or their downstream signaling components have been implicated in all human cancers; however, the role of these signaling pathways in the progression of prostate cancer has not been fully established. Agents that target these molecules with a high degree of specificity have been developed and tested in preclinical models and in clinical trials for prostate cancer with varying degrees of success.

Previous studies of HER2 overexpression in multiple cancers have reported ranges from 0% to 100% in IHC studies (39–42). These conflicting sets of data are most likely due to the use of different IHC assays and antibodies. Historically, HER2 overexpression has been determined solely by gene amplification and, because of this, protein levels of HER2 have not been extensively explored and characterized in prostate cancer progression. The histopathologic findings from this study demonstrated that the overexpression of both HER2 and EGFR proteins is associated with prostate cancer progression and bone metastasis. While *ERBB2* gene amplification does not appear to play a role in the etiology of localized prostate cancer progression (8), this had not been examined in metastatic prostate cancer. Hence, FISH analysis was used on both TMAs showing no instances of *ERBB2* gene amplification, although the amplification of *EGFR* in prostate cancer metastasis remains unreported. Therefore, overexpression of HER2 protein may be sufficient to support the osseous metastasis of human prostate cancer.

It is now believed that the RANK signaling axis may directly regulate both HER2 protein overexpression in breast cancer (28, 29) and prostate cancer bone metastasis (30, 43). In our previous study of metastatic breast cancer, we found that HER2 overexpression was not due to gene amplification but was mediated by receptor activation of RANK by RANKL (an abundant ligand in the bone microenvironment). This study also showed that HER2 is selectively expressed in the CSCs and that MCF7 cells growing in mouse tibiae express higher levels of HER2 than the same cells grown in other tissues (12). The current study demonstrates that there is a significant association between RANK and HER2 protein overexpression in human samples of prostate cancer bone metastasis, suggesting that this same signaling axis may be pertinent to the metastatic progression of both breast and prostate cancers.

In addition, we found that EGFR was overexpressed in prostate cancer cells and that high EGFR-expressing cells preferentially formed prostaspheres. The knockdown of HER2 in C4-2B cells did not affect the levels of EGFR expression. Our attempts to knockdown EGFR were lethal to prostate cancer cells, which is not surprising, as these lethal EGFR knockdowns have been observed in a number of studies (44–46). Taken together, this suggests that EGFR may function in various aspects of prostate cancer progression including tumor maintenance and self-renewal. Several lines of evidence support this view, including the previous observations that the addition of EGF to defined media promotes stem cell maintenance (47) and that the activation of EGFR increases prostasphere formation (48).

Recent studies suggest that CTCs may contain a highly enriched proportion of CSCs or at least exhibit many of the same characteristics (49). It will be critical to establish the molecular basis of the relationship between CTCs and CSCs. Of particular interest to us was the relationship between the role of EGFR in prostate TICs and survival of prostate CTCs. It is likely that diverse signaling pathways are required to maintain the cells in circulation and support them as they reestablish their growth at distant sites. There is an increasing body of evidence

suggesting that EGFR and HER2 may play such a role (50, 51). This is supported by the finding that not only is EGFR protein expressed in metastatic prostate cancer (4) but also that it is required for sphere formation in culture. Because of the described microfluidic isolation technology, we were also able to demonstrate that EGFR is expressed in CTCs of men with metastatic prostate cancer.

The pivotal role of EGFR family members in multiple cancers has led to the development of targeted therapies, including therapeutic antibodies and small-molecule inhibitors. Targeting HER2-overexpressing breast cancers with trastuzumab, the therapeutic monoclonal antibody against HER2, has been proven efficacious. Treatment of HER2-expressing CRPC with trastuzumab had little response (clinical trial report NCT00003740). However, trials using cetuximab, erlotinib, and lapatinib have shown a variety of benefits in patients with prostate cancer who express these targets (NCT00728663, NCT00272038, NCT00103194; refs. 52–54). Low patient accrual, late stage of disease, and formation of various EGFR family dimers (affecting inhibitor binding) are some of the variables that may mask the true effectiveness of these drugs. Although some of the ErbB-specific therapeutics used in this study previously failed in the clinical setting, our results warrant further consideration for repurposing these compounds in combination with other modalities or in the selection of candidates based on ErbB status.

In summary, we found that HER2 protein was elevated in CRPC bone metastasis and that HER2 expression in these same lesions may be dependent on the expression and activation of RANK. In addition, we observed that EGFR expression in bone metastasis was independent of HER2 status and was critical for sphere formation in the TIC component of these tumors and was present on the CTCs of patients with metastatic prostate cancer. The importance of HER2 and EGFR in the metastatic progression of prostate cancer was reflected in the mouse studies where only dual inhibition of both receptors inhibited tumor growth.

Disclosure of Potential Conflicts of Interest

M.L. Day reports receiving a commercial research grant from and is a consultant/advisory board member of European Egyptian Pharmaceutical Industries. No potential conflicts of interest were disclosed by the other authors.

Authors' Contributions

Conception and design: K.C. Day, G. Lorenzatti Hilles, M. Kozminsky, R. Shah, K.W. Ignatoski, E. Keller, S. Nagrath, M.L. Day

Development of methodology: K.C. Day, G. Lorenzatti Hilles, M. Kozminsky, A. Paul, C. Hall, E. Keller, D. Thomas, S. Nagrath

Acquisition of data (provided animals, acquired and managed patients, provided facilities, etc.): K.C. Day, G. Lorenzatti Hilles, M. Kozminsky, L.J. Broses, R. Shah, C. Hall, N. Palanisamy, L. El-Sawy, S.J. Wilson, K.W. Ignatoski, D. Thomas, S. Nagrath, T. Morgan

Analysis and interpretation of data (e.g., statistical analysis, biostatistics, computational analysis): K.C. Day, G. Lorenzatti Hilles, M. Kozminsky, L.J. Broses, R. Shah, L.P. Kunja, C. Hall, S. Daignault-Newton, S.J. Wilson, A. Chou, D. Thomas, S. Nagrath, T. Morgan, M.L. Day

Writing, review, and/or revision of the manuscript: K.C. Day, G. Lorenzatti Hilles, M. Kozminsky, A. Paul, L.J. Broses, L.P. Kunja, S. Daignault-Newton, L. El-Sawy, E. Keller, D. Thomas, S. Nagrath, T. Morgan, M.L. Day

Administrative, technical, or material support (i.e., reporting or organizing data, constructing databases): K.C. Day, S.J. Dawsey, A. Paul, A. Chou, S. Nagrath, M.L. Day

Study supervision: K.C. Day, R. Shah, S. Nagrath, M.L. Day

Acknowledgments

We thank the Vector, Flow Cytometry, Pathology and ULAM UMCCC core facilities and the Lurie Nanofabrication Facility at the University of Michigan for their support. We thank the Department of Radiology for the use of The Center for Molecular Imaging and the Tumor Imaging Core. Special gratitude to Danielle Fasseel and Amy Gursky.

Grant Support

The study was supported by Department of Defense PC030659 (M.L. Day), NIH R01 DK56137 (M.L. Day), NIH P01CA093900 (E. Keller), UL1TR000433 (G. Lorenzatti Hiles, Postdoctoral Translational Scholars Program, Michigan Institute for Clinical and Health Research); SPORE P50 CA186786 (A. Chinnaiyan), NSF GRFP DGE 1256260 (M. Kozminsky) and the NIH through the University of Michigan's Cancer Center Support Grant (P30 CA046592); Prostate Cancer Foundation Young Investigator Award and Department of Defense Physician Research Training Award (W81XWH-14-1-0287 to T. Morgan).

The costs of publication of this article were defrayed in part by the payment of page charges. This article must therefore be hereby marked *advertisement* in accordance with 18 U.S.C. Section 1734 solely to indicate this fact.

Received June 17, 2016; revised September 22, 2016; accepted October 18, 2016; published OnlineFirst October 28, 2016.

References

1. SEER Stat Fact Sheets: Prostate Cancer. Bethesda, MD: National Cancer Institute. Available from: https://seer.cancer.gov/statfacts/html/prost.html. Accessed November 2016.
2. DeHaan AM, Wolters NM, Keller ET, Ignatoski KM. EGFR ligand switch in late stage prostate cancer contributes to changes in cell signaling and bone remodeling. Prostate 2009;69:528–37.
3. Traish AM, Morgentaler A. Epidermal growth factor receptor expression escapes androgen regulation in prostate cancer: a potential molecular switch for tumour growth. Br J Cancer 2009;101:1949–56.
4. Shah RB, Ghosh D, Elder JT. Epidermal growth factor receptor (ErbB1) expression in prostate cancer progression: correlation with androgen independence. Prostate 2006;66:1437–44.
5. Craft N, Shostak Y, Carey M, Sawyers CL. A mechanism for hormone-independent prostate cancer through modulation of androgen receptor signaling by the HER-2/neu tyrosine kinase. Nat Med 1999;5:280–5.
6. Piccart-Gebhart MJ, Procter M, Leyland-Jones B, Goldhirsch A, Untch M, Smith I, et al. Trastuzumab after adjuvant chemotherapy in HER2-positive breast cancer. N Engl J Med 2005;353:1659–72.
7. Barthelemy P, Leblanc J, Goldbarg V, Wendling F, Kurtz JE. Pertuzumab: development beyond breast cancer. Anticancer Res 2014;34:1483–91.
8. Minner S, Jessen B, Stiedenroth L, Burandt E, Kollermann J, Mirlacher M, et al. Low level HER2 overexpression is associated with rapid tumor cell proliferation and poor prognosis in prostate cancer. Clin Cancer Res 2010;16:1553–60.
9. Lu X, Kang Y. Epidermal growth factor signalling and bone metastasis. Br J Cancer 2010;102:457–61.
10. Schramek D, Penninger JM. The many roles of RANKL-RANK signaling in bone, breast and cancer. IMBS BoneKEy 2011;8:237–56.
11. Tan W, Zhang W, Strasner A, Grivennikov S, Cheng JQ, Hoffman RM, et al. Tumour-infiltrating regulatory T cells stimulate mammary cancer metastasis through RANKL-RANK signalling. Nature 2011;470:548–53.
12. Ithimakin S, Day KC, Malik F, Zen Q, Dawsey SJ, Bersano-Begey TF, et al. HER2 drives luminal breast cancer stem cells in the absence of HER2 amplification: implications for efficacy of adjuvant trastuzumab. Cancer Res 2013;73:1635–46.
13. Palafox M, Ferrer I, Pellegrini P, Vila S, Hernandez-Ortega S, Urruticoechea A, et al. RANK induces epithelial-mesenchymal transition and stemness in

human mammary epithelial cells and promotes tumorigenesis and metastasis. Cancer Res 2012;72:2879–88.
14. Gupta GP, Massague J. Cancer metastasis: building a framework. Cell 2006;127:679–95.
15. Mehra N, Zafeiriou Z, Lorente D, Terstappen LW, de Bono JS. CCR 20th anniversary commentary: circulating tumor cells in prostate cancer. Clin Cancer Res 2015;21:4992–5.
16. Yoon HJ, Kim TH, Zhang Z, Azizi E, Pham TM, Paoletti C, et al. Sensitive capture of circulating tumour cells by functionalized graphene oxide nanosheets. Nat Nanotechnol 2013;8:735–41.
17. Kozminsky M, Wang Y, Nagrath S. The incorporation of microfluidics into circulating tumor cell isolation for clinical applications. Curr Opin Chem Eng 2016;11:59–66.
18. Dai J, Zhang H, Karatsinides A, Keller JM, Kozloff KM, Aftab DT, et al. Cabozantinib inhibits prostate cancer growth and prevents tumor-induced bone lesions. Clin Cancer Res 2014;20:617–30.
19. Molina JR, Kaufmann SH, Reid JM, Rubin SD, Galvez-Peralta M, Friedman R, et al. Evaluation of lapatinib and topotecan combination therapy: tissue culture, murine xenograft, and phase I clinical trial data. Clin Cancer Res 2008;14:7900–8.
20. Strecker TE, Shen Q, Zhang Y, Hill JL, Li Y, Wang C, et al. Effect of lapatinib on the development of estrogen receptor-negative mammary tumors in mice. J Natl Cancer Inst 2009;101:107–13.
21. Gril B, Palmieri D, Bronder JL, Herring JM, Vega-ValleF E, Feigenbaum L, et al. Effect of lapatinib on the outgrowth of metastatic breast cancer cells to the brain. J Natl Cancer Inst 2008;100:1092–103.
22. Friess T, Scheuer W, Hasmann M. Combination treatment with erlotinib and pertuzumab against human tumor xenografts is superior to monotherapy. Clin Cancer Res 2005;11:5300–9.
23. Rubin MA, Dunn R, Strawderman M, Pienta KJ. Tissue microarray sampling strategy for prostate cancer biomarker analysis. Am J Surg Pathol 2002;26:312–9.
24. Kuefer R, Day KC, Kleer CG, Sabel MS, Hofer MD, Varambally S, et al. ADAM15 disintegrin is associated with aggressive prostate and breast cancer disease. Neoplasia 2006;8:319–29.
25. Rubin MA, Putzi M, Mucci N, Smith DC, Wojno K, Korenchuk S, et al. Rapid ("warm") autopsy study for procurement of metastatic prostate cancer. Clin Cancer Res 2000;6:1038–45.
26. Gleason DF.Classification of prostatic carcinomas. Cancer Chemother Rep Part 1 1966;50:125–8.
27. Najy AJ, Day KC, Day ML. The ectodomain shedding of E-cadherin by ADAM15 supports ErbB receptor activation. J Biol Chem 2008;283:18393–401.
28. Cao N, Li S, Wang Z, Ahmed KM, Degnan ME, Fan M, et al. NF-kappaB-mediated HER2 overexpression in radiation-adaptive resistance. Radiat Res 2009;171:9–21.
29. Cao Y, Luo JL, Karin M. IkappaB kinase alpha kinase activity is required for self-renewal of ErbB2/Her2-transformed mammary tumor-initiating cells. Proc Natl Acad Sci U S A 2007;104:15852–7.
30. Chu GC, Zhau HE, Wang R, Rogatko A, Feng X, Zayzafoon M, et al. RANK- and c-Met-mediated signal network promotes prostate cancer metastatic colonization. Endocr Relat Cancer 2014;21:311–26.
31. Garraway IP, Sun W, Tran CP, Perner S, Zhang B, Goldstein AS, et al. Human prostate sphere-forming cells represent a subset of basal epithelial cells capable of glandular regeneration *in vivo*. Prostate 2010;70:491–501.
32. Portillo-Lara R, Alvarez MM. Enrichment of the cancer stem phenotype in sphere cultures of prostate cancer cell lines occurs through activation of developmental pathways mediated by the transcriptional regulator DeltaNp63alpha. PLoS One 2015;10:e0130118.
33. Rajasekhar VK, Studer L, Gerald W, Socci ND, Scher HI. Tumour-initiating stem-like cells in human prostate cancer exhibit increased NF-kappaB signalling. Nat Commun 2011;2:162.
34. Rybak AP, He L, Kapoor A, Cutz JC, Tang D. Characterization of sphere-propagating cells with stem-like properties from DU145 prostate cancer cells. Biochim Biophys Acta 2011;1813:683–94.
35. Payne RE, Yague E, Slade MJ, Apostolopoulos C, Jiao LR, Ward B, et al. Measurements of EGFR expression on circulating tumor cells are reproducible over time in metastatic breast cancer patients. Pharmacogenomics 2009;10:51–7.
36. Pestrin M, Bessi S, Galardi F, Truglia M, Biggeri A, Biagioni C, et al. Correlation of HER2 status between primary tumors and corresponding circulating tumor cells in advanced breast cancer patients. Breast Cancer Res Treat 2009;118:523–30.
37. Riethdorf S, Muller V, Zhang L, Rau T, Loibl S, Komor M, et al. Detection and HER2 expression of circulating tumor cells: prospective monitoring in breast cancer patients treated in the neoadjuvant GeparQuattro trial. Clin Cancer Res 2010;16:2634–45.
38. Shaffer DR, Leversha MA, Danila DC, Lin O, Gonzalez-Espinoza R, Gu B, et al. Circulating tumor cell analysis in patients with progressive castration-resistant prostate cancer. Clin Cancer Res 2007;13:2023–9.
39. Scher HI, Sarkis A, Reuter V, Cohen D, Netto G, Petrylak D, et al. Changing pattern of expression of the epidermal growth factor receptor and transforming growth factor alpha in the progression of prostatic neoplasms. Clin Cancer Res 1995;1:545–50.
40. Jorda M, Morales A, Ghorab Z, Fernandez G, Nadji M, Block N. Her2 expression in prostatic cancer: a comparison with mammary carcinoma. J Urol 2002;168:1412–4.
41. Chow NH, Chan SH, Tzai TS, Ho CL, Liu HS. Expression profiles of ErbB family receptors and prognosis in primary transitional cell carcinoma of the urinary bladder. Clin Cancer Res 2001;7:1957–62.
42. Jimenez RE, Hussain M, Bianco FJ Jr, Vaishampayan U, Tabazcka P, Sakr WA, et al. Her-2/neu overexpression in muscle-invasive urothelial carcinoma of the bladder: prognostic significance and comparative analysis in primary and metastatic tumors. Clin Cancer Res 2001;7:2440–7.
43. Chu GC, Chung LW. RANK-mediated signaling network and cancer metastasis. Cancer Metastasis Rev 2014;33:497–509.
44. Weihua Z, Tsan R, Huang WC, Wu Q, Chiu CH, Fidler IJ, et al. Survival of cancer cells is maintained by EGFR independent of its kinase activity. Cancer Cell 2008;13:385–93.
45. Mueller KL, Yang ZQ, Haddad R, Ethier SP, Boerner JL. EGFR/Met association regulates EGFR TKI resistance in breast cancer. J Mol Signal 2010;5:8.
46. Miettinen PJ, Berger JE, Meneses J, Phung Y, Pedersen RA, Werb Z, et al. Epithelial immaturity and multiorgan failure in mice lacking epidermal growth factor receptor. Nature 1995;376:337–41.
47. Litvinov IV, Vander Griend DJ, Xu Y, Antony L, Dalrymple SL, Isaacs JT. Low-calcium serum-free defined medium selects for growth of normal prostatic epithelial stem cells. Cancer Res 2006;66:8598–607.
48. Rybak AP, Ingram AJ, Tang D. Propagation of human prostate cancer stem-like cells occurs through EGFR-mediated ERK activation. PLoS One 2013;8:e61716.
49. Azizi E, Nagrath S, Kozminsky M, Wicha MS. Circulating tumor cells. Cole RJ, Datar RH, editors. New York: Springer-Verlag; 2016. p. 333.
50. Dittrich A, Gautrey H, Browell D, Tyson-Capper A. The HER2 signaling network in breast cancer–like a spider in its web. J Mammary Gland Biol Neoplasia 2014;19:253–70.
51. Yeo SK, Wen J, Chen S, Guan JL. Autophagy differentially regulates distinct breast cancer stem-like cells in murine models via EGFR/Stat3 and Tgfbeta/Smad signaling. Cancer Res 2016;76:3397–410.
52. Cathomas R, Rothermundt C, Klingbiel D, Bubendorf L, Jaggi R, Betticher DC, et al. Efficacy of cetuximab in metastatic castration-resistant prostate cancer might depend on EGFR and PTEN expression: results from a phase II trial (SAKK 08/07). Clin Cancer Res 2012;18:6049–57.
53. Nabhan C, Lestingi TM, Galvez A, Tolzien K, Kelby SK, Tsarwhas D, et al. Erlotinib has moderate single-agent activity in chemotherapy-naive castration-resistant prostate cancer: final results of a phase II trial. Urology 2009;74:665–71.
54. Liu G, Chen YH, Kolesar J, Huang W, Dipaola R, Pins M, et al. Eastern Cooperative Oncology Group Phase II Trial of lapatinib in men with biochemically relapsed, androgen dependent prostate cancer. Urol Oncol 2013;31:211–8.